Isolation and Screening of Indigenous Filamentous Fungi Producing Ligninolytic, Cellulolytic and Hemicellulolytic Enzymes from Decomposed Oil Palm Frond

Ahmad Fariz Nicholas[1], Hasliza Abu Hassim[1,2]*, Mohd Huzairi Mohd Zainudin[2], Zunita Zakaria[1], Mohd Termizi Yusof[3], Mohd Nazri Md Nayan[4] and Amirul Faiz Mohd Azmi[5]

[1]*Department of Veterinary Preclinical Sciences, Faculty of Veterinary Medicine, Universiti Putra Malaysia, 43400 UPM, Serdang, Selangor, Malaysia*
[2]*Laboratory of Sustainable Animal Production and Biodiversity, Institute of Tropical Agriculture and Food Security, Universiti Putra Malaysia, 4300 UPM, Serdang, Selangor, Malaysia*
[3]*Department of Microbiology, Faculty of Biotechnology and Biomolecular Sciences, Universiti Putra Malaysia, 43400 UPM, Serdang, Selangor, Malaysia*
[4]*Department of Animal Science, Universiti Putra Malaysia, 43400 UPM, Serdang, Selangor, Malaysia*
[5]*Department of Veterinary Preclinical Sciences, Faculty of Veterinary Medicine, Universiti Malaysia Kelantan, 16100 Kota Bharu, Kelantan, Malaysia*

ABSTRACT

Oil palm frond (OPF) is a palm oil plantation by-product commonly used in animal feeding in Malaysia. The large production, availability, and nutrient content make OPF the best candidate for utilization as animal feed. However, OPF contains high lignin bonds to cellulose and hemicellulose that further limit the digestibility of rumen microbes to produce volatile fatty acids as an energy source for ruminants. This study aims to identify and determine the enzyme activity (ligninolytic, cellulolytic, and hemicellulolytic) of enzymes extracted from filamentous fungi in the pre-treatment of OPF using the solid-state fermentation (SSF) technique. The enzyme extracted from SSF was determined by its enzyme activity (laccase, lignin peroxidase, manganese peroxidase, carboxymethylcellulose, avicelase, and xylanase). Eight fungi were successfully identified to produce enzymes determined in this experiment. *Phanerina mellea* showed the highest average ligninolytic enzyme activity with a value of 0.37 U/mL and an average cellulolytic + hemicellulolytic of

Ahmad Fariz Nicholas, Hasliza Abu Hassim, Mohd Huzairi Mohd Zainudin, Zunita Zakaria,
Mohd Termizi Yusof, Mohd Nazri Md Nayan and Amirul Faiz Mohd Azmi

0.18 U/mL. In this experiment, *P. mellea* was the most desired fungi for the pre-treatment of OPF. The optimum ligninolytic enzyme production time of OPF pre-treatment is 10 days of SSF.

Keywords: Animal feed, biological pre-treatment, enzyme activity, lignin, oil palm frond, white rot fungi

INTRODUCTION

The abundant lignocellulosic materials from either agriculture or forestry wastes triggered various applications to utilize and turn scraps into valuable products (Manavalan et al., 2015). In Malaysia, oil palm plantations represent 60% of total agricultural land, contributing to high lignocellulosic waste materials (Ghani et al., 2017). The planted area of palm oil trees in Malaysia for 2022 is 5.67 million hectares, which is 1.1% lower compared to 5.74 million hectares in 2021 (Parveez et al., 2022). However, the reduced planted area is caused by the replanting of the trees, and the numbers will be increased, directly increasing the amount of OPF production in Malaysia. The valorization of lignocellulosic waste materials becomes the subject of intense study since they are potentially harmful to the environment.

Lignocellulosic material like oil palm frond (OPF) is a carbohydrate-rich residue containing significant cellulose, hemicellulose and lignin (Sukri et al., 2014). OPF contains 22% soluble carbohydrate and 70% fiber on a dry matter (DM) basis (Saminathan et al., 2012). According to Islam et al. (2000), the nutritional composition of OPF is 439, 926, 698, 501, 168, 196, 748, and 52 (g/kg) of DM, organic matter (OM), neutral detergent fiber (NDF), acid detergent fiber (ADF), cellulose, hemicellulose, total carbohydrate (TC), and non-fiber carbohydrate (NFC), respectively for leaflet parts of the OPF. At the same time, the petiole contains lower (p<0.01) DM, CP and EE than the leaflet (Islam et al., 2000).

As a substitute for grasses or roughages, OPF is commonly used as ruminant feed, especially during the short feed supply (Rusli et al., 2019). The potential of OPF to be livestock feed is hindered by the high neutral detergent fiber (NDF)and lignin contents of the OPF itself (Rahman et al., 2011), making it difficult to be degraded by ruminant digestive systems. To overcome this problem, various pre-treatment methods, such as enzymatic treatment, have been used to improve the digestibility of lignocellulose materials in ruminant feed.

White rot fungi (WRF) is a decaying wood fungus in agricultural residues. It can leave a remarkable reaction by leaving a bleached on the attacked wood by lignin degradation (Asgher et al., 2008). The valuable enzyme system of WRF and its effectiveness in degrading lignocellulosic biomasses attracted considerable research interest in different fields of study (Manavalan et al., 2015). The lignin-degrading capabilities of WRF inspired studies to deepen the knowledge of its enzyme activity for various importances. Many species have been studied, including *Ceriporiopsis subvermispora* (Rahman et al., 2011), *Pleurotus ostreatus* (Tuyen et al., 2013), and *Lentinussajor-caju* (Chanjula et al.,

2017). However, less than 20 species out of 1500 different species of WRF were applied in biological pre-treatment. There are possibilities that the potential WRF can be found in nature (Tian et al., 2012).

Three major enzymes that are working in the degradation of lignin produced by WRF are laccase, lignin peroxidase (LiP), and manganese peroxidase (MnP) (Robinson et al., 2001). These ligninolytic enzymes mineralize the lignin into carbon dioxide (CO_2) and water. These enzymes were used in various applications, for example, bleaching and wastewater treatment for laccase enzyme (Madhavi & Lele, 2009), coal depolymerization and skin lightening by melanin oxidation for LiP enzyme (Falade et al., 2017), and juice extract clarification and biofuel production for MnP enzyme (Kumar & Arora, 2022). The delignification of the lignocellulosic biomasses will allow more cellulose and hemicellulose release for rumen microbial activity. Accessing rumen microbes to cellulose and hemicellulose is the key to improving rumen degradability (Rusli et al., 2021).

The study on the effect of pre-treated OPF feeding on meat quality and animal performance is minimal. A study reported by Azmi et al. (2019) showed that the nutritional value of OPF can be improved by pre-treating it with ligninolytic enzyme extract. Another study reported by Hamchara et al. (2018) showed that the feeding of OPF pre-treated with *L. sajor*-ceju to 16-month-old crossbred male goats improved the estimated energy intakes (ME Mcal/DM/d) by up to 53 %. The pre-treatment of OPF by WRF is promising in improving the low nutritional value of OPF. This study aims to identify and determine the enzyme activity of enzyme extract from filamentous fungi collected from Palm oil tree plantations in Taman Pertanian Universiti, Universiti Putra Malaysia (TPU, UPM).

MATERIALS AND METHODS

Fungi Culture and Isolation

The fungi were collected at the Palm oil tree plantations in University Agricultural Park, Universiti Putra Malaysia (UAP, UPM) (2.983592895423529, 101.71000476197045). The fungi were collected from rotten oil palm fronds, placed in paper bags, and taken to the FAMTEC laboratory in the Faculty of Biotechnology UPM (Azmi et al., 2019). The collected samples were cultured on potato dextrose agar (PDA) (Bacton, Dickinson and Company, USA) containing streptomycin and penicillin antibiotics. The sub-culturing process was repeated until the pure culture was obtained. Stocks of isolated fungi were prepared using the filter paper method and agar slant.

Morphological Identification

The isolated fungi were cultured on PDA (OXOID CM0139) agar for seven days before being used for microscopic observation and identification. First, the morphology of the

fungi on the agar plate was observed. The culture's texture, structure, edge, and elevation were also observed.

Molecular Identification

The DNA extracted from the isolated fungi underwent a polymerase chain reaction (PCR) using Bio-Rad T100 PCR Thermal Cycler with primer internal transcribed spacer, ITS1 (5'-TCCGTAGGTGAACCTGCGG-3') and ITS4 (5'-TCCTCCGCTTATTGATATGC-3'). ITS1 and ITS4 acted as forward and reversed primers, respectively. The amplified DNA was run on gel electrophoresis and viewed under UV light with the range size of 600 and 700 base pairs (bp). The sequencing was done, and the Apical Scientific (1st Base) result was processed with Chromas and MEGA7 software. The aligned sequence was compared with the sequence in GenBank using the Basic Local Alignment Search Tool (BLAST), NCBI, and the fungal species were determined. The phylogenetic tree was constructed using NCBI taxonomy and MEGA7 software.

Microscopic Observation

The fungi were placed onto a glass slide covered with a cover slip and pressed to get a good separation of the hyphae. A methylene blue solution was used for staining. The fungi characteristics were then observed using a compound microscope (Olympus BX53M, Japan) with a digital camera. The morphological structure of the fungi was compared with the previous studies and determined based on fungi characteristics stated by Galal et al. (2017). The characteristics involve branching, hyphae, conidiospores and spores (Galal et al., 2017).

Solid-state Fermentation

The OPF was collected from Taman Pertanian Universiti, Universiti Putra Malaysia. Then, the OPF was chopped into a smaller size. In the Erlenmeyer flask, 15 g of chopped OPF was added. Then, 0.05% of glucose and 2.4 mM of nitrogen source, ammonium sulfate $((NH_4)_2SO_4)$, were added to 45 mL of distilled water. The flasks were then covered with cotton plugs and aluminum foil. It was autoclaved to remove any existing microorganisms. Each flask was added with three 3–10 mm agar plugs from each fungi culture. The flasks were incubated in the oven incubator at 28°C for 10, 20, and 30 days (Azmi et al., 2019).

Enzyme Extraction

Enzyme extraction begins once the fermentation period ends. Each flask received 150 mL of distilled water, and the flasks were shaken for 3 hours. The mixture was then filtered

using six layers of wound gauze. The filtrate was mixed with polyvinylpolypyramidone (PVPP) to remove tannins (Toth & Pavia, 2000). The amount of PVPP added is 0.5% of the total filtrate. The mix of the filtrate and PVPP was centrifuged (Avanti J-26S XP1, High-Performance Centrifuge, Beckman Coulter, USA) at 12,000 g for 10 minutes. The temperature during the centrifuging process was 4°C. The supernatant was then collected and stored for enzyme activity determination (Azmi et al., 2019).

Ligninolytic Enzyme Activity Determinations

Laccase enzyme activity determination used citrate-phosphate buffer and 2,2'-azino-bis(3-ethylbenzothiazoline-6-sulphonic (ABTS) acid substrate in the experiment. To prepare citrate-phosphate buffer (50 mM), 1.921 g of citric acid, $C_6H_8O_7$, was added into 100 ml distilled water and the pH was calibrated to pH 5.0 and labeled as solution A. Then, 3.581 g of sodium phosphate dibasic, Na_2HPO_4, was added into 100 mL distilled water and labeled solution B. The substrate was prepared with 0.165 g of ABTS added into 10 mL of distilled water. The substrate was then transferred to an Eppendorf tube. The blank solution was prepared before reading at 420 nm light absorbance of spectrophotometer nanodrop (Tecan Infinite M200 Pro™, Switzerland) against blank. All enzyme activity values were represented in unit concentration, U/mL (unit/milliliter), with three replicates (Azmi et al., 2019). The calculation for laccase enzyme activity determination was done using Equation 1.

$$\text{Concentration} \left(\frac{\text{U}}{\text{ml}}\right) = \frac{A}{\Sigma \text{mM}^{-1}\text{cm}^{-1}} \times \frac{1500 \text{ ul}}{100 \text{ ul}} \qquad [1]$$

Where A = Absorbance; total volume in cuvette = 1500 ul; total volume of enzyme in cuvette = 100 ul; and light absorbance at 420 nm = Σ mM^{-1} cm^{-1}

Lignin peroxidase enzyme activity was determined with acid tartrate buffer, substrate, and hydrogen peroxide, H_2O_2 used in the experiment. The buffer was prepared with 3.752 g of acid tartrate, $C_4H_6O_6$ was added to 250 mL of distilled water, and the pH was calibrated to pH 3.0 with HCL before being kept at 4°C. Substrate preparation was done with 0.105 mL of veratryl alcohol (3, 4-Dimethoxybenzyl alcohol) added to 25 mL of distilled water and stored at 4°C in an Eppendorf tube. Then, the hydrogen peroxide, H_2O_2, was prepared according to the manufacturer's specifications. After that, the mixture tube was prepared by adding 2570 µL of acid tartrate buffer, 200 µL veratryl alcohols, 30 µL hydrogen peroxide, and 200 µL of enzyme extract. The blank prepared with 2570 µL of acid tartrate buffer was added to 200 µL veratryl alcohol and 30 µL hydrogen peroxide. Finally, the mixture tubes were read at 310 nm light absorbance of spectrophotometer nanodrop (Tecan Infinite M200 Pro™, Switzerland) against blank. The calculation for LiP enzyme activity determination was done using Equation 2.

Ahmad Fariz Nicholas, Hasliza Abu Hassim, Mohd Huzairi Mohd Zainudin, Zunita Zakaria,
Mohd Termizi Yusof, Mohd Nazri Md Nayan and Amirul Faiz Mohd Azmi

$$\text{Concentration } \left(\frac{U}{ml}\right) = \frac{A}{\Sigma mM^{-1}cm^{-1}} \times \frac{3000 \text{ ul}}{200 \text{ ul}} \qquad [2]$$

Where: A = Absorbance; total volume in cuvette = 1500 uL; total volume of enzyme in cuvette = 100 uL; light absorbance at 310 nm = Σ mM^{-1} cm^{-1}

Manganese peroxidase was determined by preparing a sodium tartrate buffer with 5.752 g of sodium tartrate added to 250 mL of distilled water. The solution was adjusted to pH 5.0 using HCL or NaOH and kept at 4°C. The substrate was prepared by adding 0.254 g of manganese sulfate to 50 ml of distilled water and stored at 4°C. The H_2O_2 was prepared according to the manufacturer's specifications. After that, the mixture tube was prepared by adding 2550 µL of sodium tartrate buffer mixed with 200 µL manganese sulfate, 30 µL H_2O_2, and 200 µL of enzyme extract. The blank was prepared by 2550 µL sodium tartrate buffer added to 200 µL manganese sulfate and 30 µL H_2O_2. The mixture tubes were read at 238 nm light absorbance of spectrophotometer nanodrop (Tecan Infinite M200 Pro™, Switzerland) against blank. The calculation for MnP enzyme activity determination was done using Equation 3.

$$\text{Concentration } \left(\frac{U}{ml}\right) = \frac{A}{\Sigma mM^{-1}cm^{-1}} \times \frac{3000 \text{ ul}}{200 \text{ ul}} \qquad [3]$$

Where: A = Absorbance; total volume in cuvette = 1500 uL; total volume of enzyme in cuvette = 100 uL; light absorbance at 238 nm = Σ mM^{-1} cm^{-1}

Cellulolytic Enzyme Activity Determination

Substrate and citrate buffers were prepared to screen carboxylmethylcellylase (CMCase) enzyme activity. The substrate was prepared with 1 g of carboxymethylcellulose and added to 100 mL of distilled water in a 250 mL Erlenmeyer flask. The solution was then stirred until homogeneous and stored at 4°C. For the citrate buffer, 0.1 M citrate buffer was prepared by adding 0.1 mol of citric acid to 0.1 mol of sodium citrate adjusted to pH 4.8 using HCl or NaOH. After that, the mixture tube was prepared by adding 0.5 mL substrate and 0.5 mL enzyme. Three control tubes were prepared: buffer control tube, enzyme control tube, and substrate control tube. For the buffer control tube, 1 mL citrate buffer in a tube was prepared. For the enzyme control tube, 0.5 ml of the enzyme was added to 0.5 mL citrate buffer and 0.5 mL of the substrate was added to 0.5 mL citrate buffer to prepare the substrate control tube. The tubes were then incubated in a water bath at 50°C for 30 min (Dinis et al., 2009). The reaction was stopped by adding 3 mL of dinitrosalicylic (DNS) acid to each tube. The mixture, buffer control, enzyme control and substrate control tubes were then placed in boiling water for 10 min. The tubes were then read at 575 nm light absorbance of spectrophotometer nanodrop (Tecan Infinite M200 Pro™, Switzerland) against blank. The glucose solution was prepared in 6 different concentrations (100 mg, 300 mg, 600 mg,

900 mg, 1200 mg, and 1500 mg) with distilled water dilution as the standard. The enzyme activity was eventually measured in unit U/mL (unit/milliliter)

Avicelase enzyme activity was determined using an avicel microcrystalline substrate and citrate buffer. Substrate of 1 g of avicel microcrystalline was used and added to 100 mL distilled water in a 250 mL Erlenmeyer flask. The solution was then stirred until homogeneous. The citrate buffer was prepared by adding 0.1 mol of citric acid with 0.1 mol of sodium citrate to get 0.1 M of citrate buffer at pH adjusted to pH 4.8, either HCl or NaOH. The mixture tube was prepared by adding 0.5 mL enzyme and 1.0 mL substrate. For the buffer control tube, 1.5 mL of citrate buffer was prepared. For the enzyme control tube, 0.5 mL of the enzyme was added to 1.0 mL citrate buffer in the tube, and for the substrate control tube, 1.0 mL substrate was added to 0.5 mL citrate buffer. The tubes were then incubated in a water bath at 50°C for 30 min (Dinis et al., 2009). The reaction was stopped by adding 3 mL of dinitrosalicylic (DNS) acid to each tube. All tubes were then placed in boiling water for 10 min. The tubes were then read at 575 nm light absorbance of spectrophotometer nanodrop (Tecan Infinite M200 Pro™, Switzerland) against blank. The glucose solution was prepared in six different concentrations (100 mg, 300 mg, 600 mg, 900 mg, 1200 mg, and 1500 mg) with distilled water dilution as the standard. The enzyme activity was eventually measured in unit U/mL (unit/milliliter)

Hemicellulolytic Enzymes Activity Determinations

This experiment added 0.25 g xylan from beechwood to 100 mL distilled water as the substrate. The solution was then heated at 70°C with continuous shaking. The citrate buffer was prepared by adding 0.1 mol of citric acid with 0.1 mol of sodium citrate to get 0.1 M of citrate buffer at pH adjusted to pH 4.8, either HCl or NaOH. The mixture tube was prepared by adding 0.5 mL enzyme to 0.5 mL substrate. The buffer control tube was prepared with only 1.0 mL citrate buffer. For the enzyme control tube, 0.5 mL enzyme was added to 0.5 mL citrate buffer and the substrate control tube was prepared by adding 0.5 mL substrate to 0.5 mL citrate buffer. The tubes were then incubated in a water bath at 50°C for 30 min (Dinis et al., 2009). The reaction was stopped by adding 3 mL of dinitrosalicylic (DNS) acid to each tube. All tubes were then placed in boiling water for 10 min. The tubes were then read at 575 nm light absorbance of spectrophotometer nanodrop (Tecan Infinite M200 Pro™, Switzerland) against blank. The xylose solution was prepared in six different concentrations (100 mg, 300 mg, 600 mg, 900 mg, 1200 mg and 1500 mg) with citrate buffer dilution as the standard.

Fungi Selection with Optimum Enzyme Activity and Pre-treatment Time

The enzyme activity determination results data were used to select fungi with the most optimum ligninolytic enzyme activity. A scatterplot graph consists of the y-axis representing

the average of total ligninolytic activity while the x-axis represents the constructed cellulolytic and hemicellulolytic average enzyme activity. The fungi that produced the high ligninolytic enzyme (laccase, LiP, and MnP) activity with low cellulolytic (CMCase and avicelase) and hemicellulolytic (xylanase) enzyme activity were selected. The optimum pre-treatment time of OPF was determined based on enzyme activity results on days 10, 20, and 30 of solid-state fermentation.

Statistical Analysis

IBM SPSS statistics 27 was used in this study and presented as mean ± SEM (standard error of the mean). Analysis of variance (ANOVA) was applied to compare the significant difference of each pre-treatment time with a significant difference of $p < 0.05$, followed by Tukey's test.

RESULTS

Morphological Selection

In this experiment, 79 fungi isolates were identified and labeled as F01 until F79. The isolates were classified into eight groups based on their morphology on the PDA agar. One isolate was selected from each group, which is F14, F03, F32, F39, F49, F65, F77, and F02 (Figure 1). All fungi were selected from the filamentous structures on the PDA agar. The fungi colony showed in white concentric rings for F14, F39, F49, and F02. The colony for F03 and F32 were green in color. F65 was brownish peach cottony, and F77
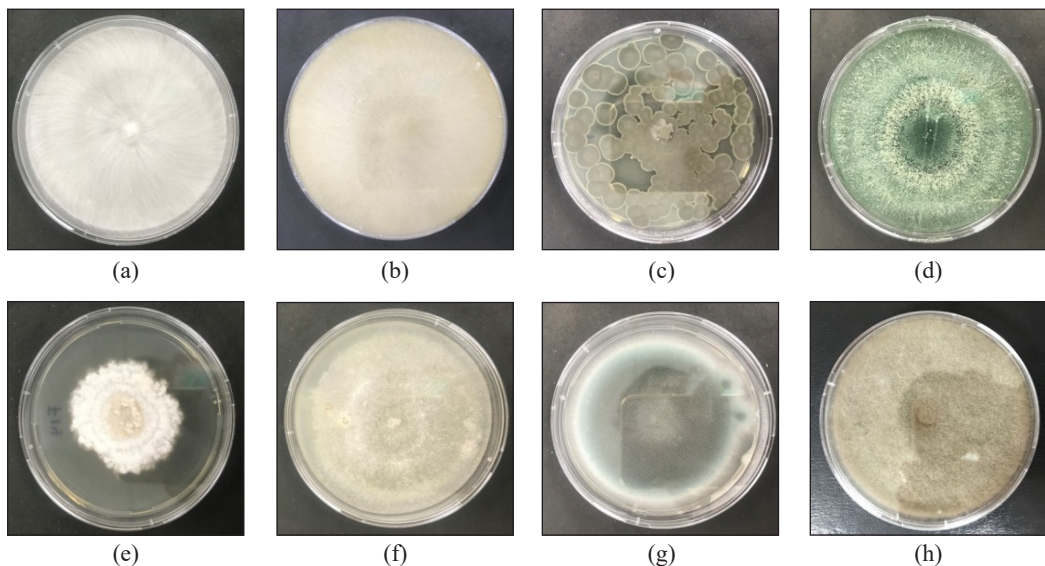

Figure 1. Selected fungi culture from eight different groups: (a) F49; (b) F02; (c) F77; (d) F32; (e) F14; (f) F39; (g) F03; and (h) F6

showed multiple scattered colonies with grey-green color rings. The fungi were also in an augmented raised cottony structure with abundant aerial mycelium grown on PDA agar (Table S1).

Molecular Observation

After a series of DNA extraction, amplification, and sequencing, the phylogenetic tree showed that the fungi were identified as F49 (*Marasmius palmivorus* MN871732), F02 (*Mucor fusiformis* KY560315), F77 (*Penicillium citrinum* MK312421), F32 (*Trichoderma asperellum* MK928414), F14 (*Schizophyllum commune* MN856258), F39 (*Phanerina mellea* or Ceriporia mellea MK432982), F03 (*Aspergillus ellipticus* MG596660) and F65 (*Syncephalastrum racemosum* MH857909) (Table S2).

Microscopic Observation

Figure 2 shows the morphology of each selected fungus under microscopic observation. The microscopic observation was based on branching, hyphae, conidiospores and spores, following Galal et al. (2017). The structures were compared with those of previous studies, as shown in Tables S3 to S10.

Schizophyllum commune showed the appearance of hyphae, and these fungi formed a clamp connection at the septa (Sigler et al., 1999). The hyphae also formed a thread-like branching and septate. However, the conidiophores and spores could not be seen. For *A. ellipticus*, it was confusing to differentiate from other *Aspergillus* sp. as the shapes were almost the same. However, *A. ellipticus* conidia were elliptical (Mahmood & Azhar, 2017). *A. ellipticus* cannot be seen clearly under the compound microscope, but the multiple conidia showed that the fungi were *Aspergillus* sp.

Trichoderma asperellum showed a branch structure with septate hypha. The conidia could be seen near the conidiophores at the tip of the hyphae. The structure was similar to that of *T. asperellum* observed by Podder and Ghosh (2019). *Phanerina mellea* hyphae structure was monomitic, brunching with a sharp angle and simple septa (Miettinen et al., 2016). The conidiophores could not be seen, and the fungi formed no clamp.

Marasmius palmivorus showed hypha with a thread-like structure under x1000 magnification of a compound microscope. The image by Tamur et al. (2019) in Table S7 showed the septal wall of fungal hyphae with the clamp connection between hyphae, which was also shown by the microscopic observation of *M. palmivorus*. The branched rough hypha structure was absent of conidiophores. *S. racemosum* could be seen, and the structure was very similar to the image shown by Raju et al. (2020) in Table S8. The conidiophores were shown in sporangiophores, and the hyphae were shown in broad aseptate.

Penicillium citrinum showed a microscopic structure similar to the image shown by Saif et al. (2020). Like other *Penicillium sp.*, *P. citrinum* contained highly branched

septate hyphae. At the tip of the hyphae, there were branches of conidiophores, the main dispersal route for the fungi. The sporangiospores structure of *M. fusiformis* could be seen under the compound microscope. However, the conidiophores could be seen clearly like the image shown by Walther et al. (2013), which was viewed using a scanning electron microscope (SEM). *Mucor fusiformis,* also known as *Zygorhynchus psychrophilus*, is in a *Mucor* group with a sporangiopores structure that is poorly sympodially branched tall with small sporangia (Walther et al., 2013).
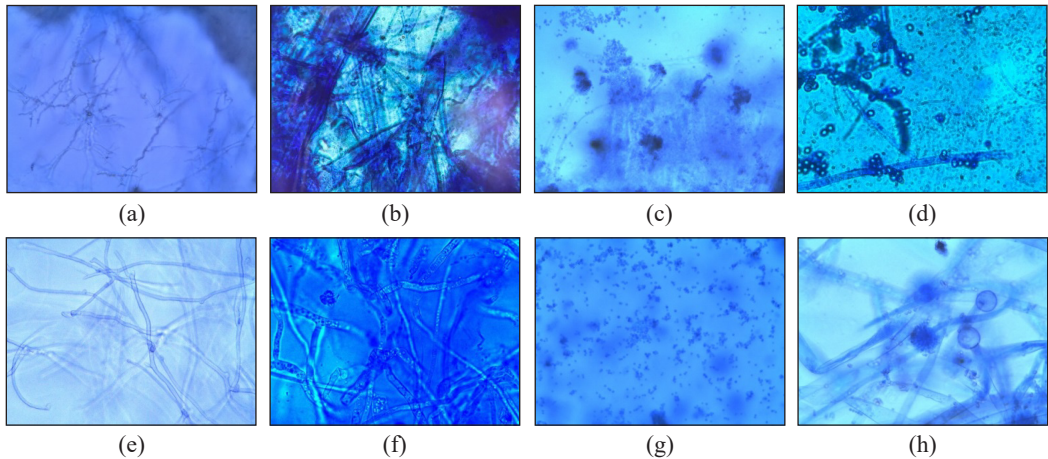
Figure 2. Microscopic morphology of eight different fungi identified: (a) *Marasmius palmivorus* (MP), (b) *Mucor fusiformis* (MF), (c) *Penicillium citrinum* (PC), (d) *Trichoderma asperellum* (TA), (e) *Schizophyllum commune* (SC), (f) *Phanerina mellea* (PM), (g) *Aspergillus ellipticus* (AE), and (h) *Syncephalastrum racemosum* (SR)

Enzyme Activity Determination

The enzyme activity determination experiment showed that all eight species of fungi identified were successfully detected to produce the enzyme analyzed in this experiment. Only *M. fusiformis* (MF) and *A. ellipticus* (AE) showed no laccase enzyme activity production.

The laccase enzyme activity of *P. mellea* (PM) showed significantly ($p<0.05$) higher average enzyme activity compared to the other fungi (Figure 3). The laccase enzyme activity of *P. mellea* increased from 0.28 U/mL on day 10 to 0.53 U/mL on day 20 of SSF. On day 30, the laccase enzyme activity of *P. mellea* decreased to 0.24 U/mL. It is followed by *M. palmivorus* (MP), *S. commune* (SC), *P. citrinum* (PC), *T. asperellum* (TA), and *S. racemosum* (SR). Most fungi, such as PM, MP, SC, PC, and TA, generally showed the highest laccase enzyme activity on day 20 of SSF.

All fungi produced lignin peroxidase (LiP) enzyme activity (Figure 4). The LiP enzyme activity of PM showed the highest value, which is 0.90 U/mL, on day 10 of SSF, compared to the other fungi. The LiP enzyme activity was then reduced to 0.34 U/mL and

0.08 U/mL on days 20 and 30 of SSF, respectively. AE, SC, SR, PC, MF, TA, and MP follow the same trend. Most fungi showed the highest LiP enzyme activity on day 10 of SSF, including PM, AE, SC, SR and PC. MF, TA, and MP showed the highest LiP enzyme activity on day 20 of SSF.

All fungi are shown to produce manganese peroxidase (MnP) enzyme activity (Figure 5). The MnP enzyme activity of SC is 0.58 U/mL on day 10 of SSF, showing the highest value, followed by AE, PM, MF, PC, TA, SR and MP. The SC MnP enzyme activity shows a decrease of 0.03 U/mL on day 20 with a value of 0.55 U/mL and decreased again to 0.39 U/mL on day 30 of SSF. Most fungi were shown to produce the highest MnP enzyme activity on day 10 of SSF except for AE and SR, which produced the highest on day 20 of SSF.

The carboxymethylcellulose (CMCase) enzyme activity for all fungi showed a similar pattern as the activity increased from day 10 to 20, setting the highest activity before reducing on day 30 of SSF (Figure 6). The CMCase enzyme activities for all fungi are the highest on day 20 of SSF compared to days 10 and 30. MF shows the highest value, 0.20 U/mL, and PC shows the lowest value, 0.02 U/mL, on day 30 of SSF.

The avicelase enzyme activity was produced by all fungi, with most fungi having the highest activity on day 20 of SSF (Figure 7). Each fungus can see no obvious comparison in a similar pattern to CMCase enzyme activity. The highest avicelase enzyme activity is shown by TA, with a value of 0.38 U/mL on day 20 of SSF, and the lowest is by AE, with a value of 0.15 U/mL on day 10 of SSF.

Xylanase enzyme activity is similar for each fungus, where the highest activity is shown on day 10 before it is reduced on days 20 and 30 of SSF (Figure 8). All fungi show a similar pattern of xylanase enzyme activity, where TA shows the highest value on day 10 with a value of 0.27 U/mL.
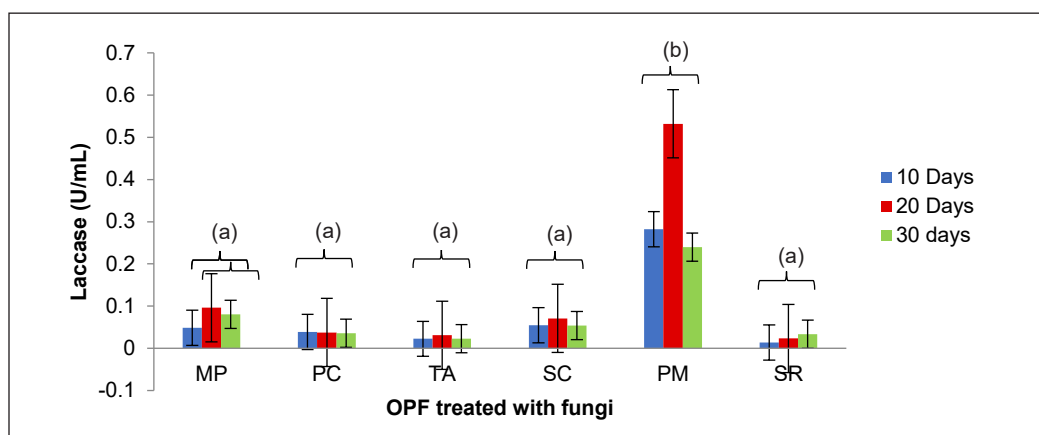

Figure 3. Laccase activity of enzyme extract after OPF pre-treatment with different fungi at 10, 20 and 30 days of incubation
Note. MP = *Marasmius palmivorus;* PC = *Penicillium citrinum;* TA = *Trichoderma asperellum;* SC = *Schizophyllum commune;* PM = *Phanerina mellea;* SR = *Syncephalastrum racemosum*

Ahmad Fariz Nicholas, Hasliza Abu Hassim, Mohd Huzairi Mohd Zainudin, Zunita Zakaria,
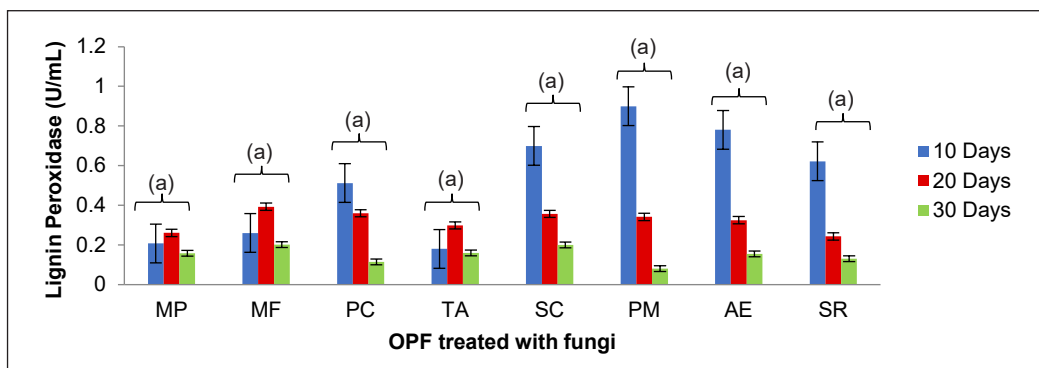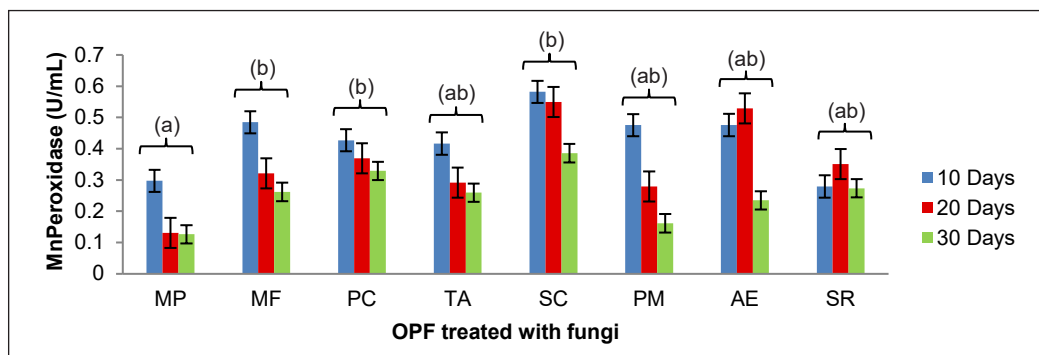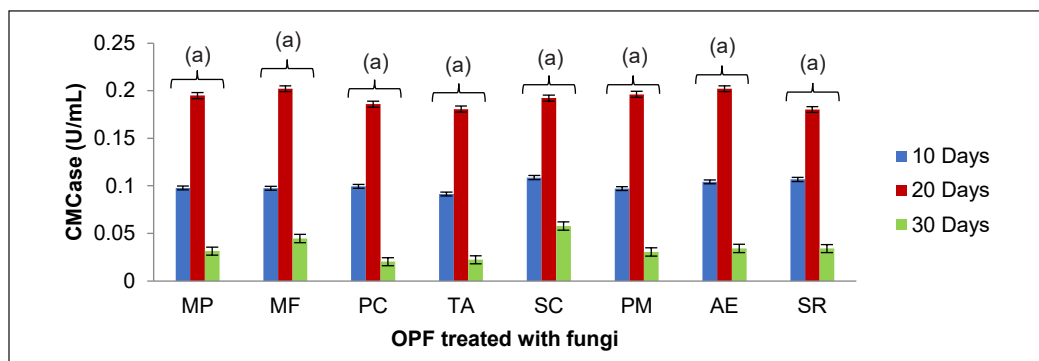Mohd Termizi Yusof, Mohd Nazri Md Nayan and Amirul Faiz Mohd Azmi

Figure 4. Lignin peroxidase activity of enzyme extract after OPF pre-treatment with different fungi at 10, 20 and 30 days of incubation (MP = *Marasmius palmivorus;* MF = *Mucor fusiformis*; PC = *Penicillium citrinum*; TA = *Trichoderma asperellum;* SC = *Schizophyllum commune;* PM = *Phanerina mellea;* AE = *Aspergillus ellipticus*; SR = *Syncephalastrum racemosum*)
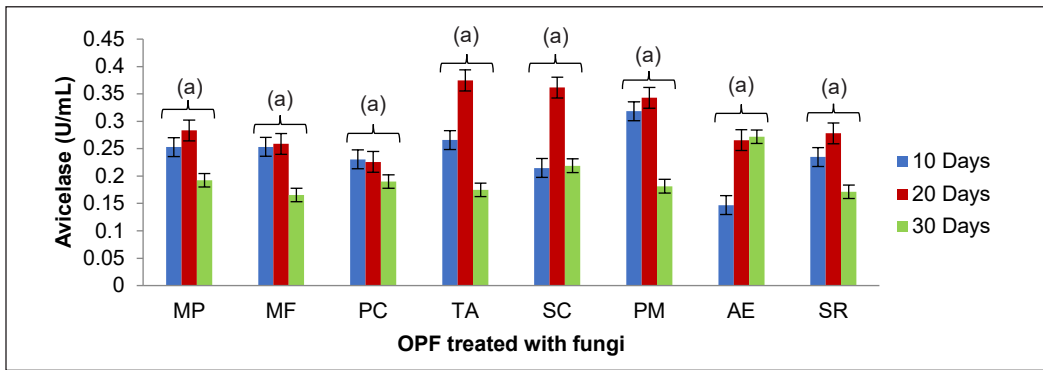

Figure 5. Manganase peroxidase activity of enzyme extract after OPF pre-treatment with different fungi at 10, 20 and 30 days of incubation (*Note.* MP = *Marasmius palmivorus;* MF = *Mucor fusiformis*; PC = *Penicillium citrinum*; TA = *Trichoderma asperellum;* SC = *Schizophyllum commune;* PM = *Phanerina mellea;* AE = *Aspergillus ellipticus*; SR = *Syncephalastrum racemosum*)
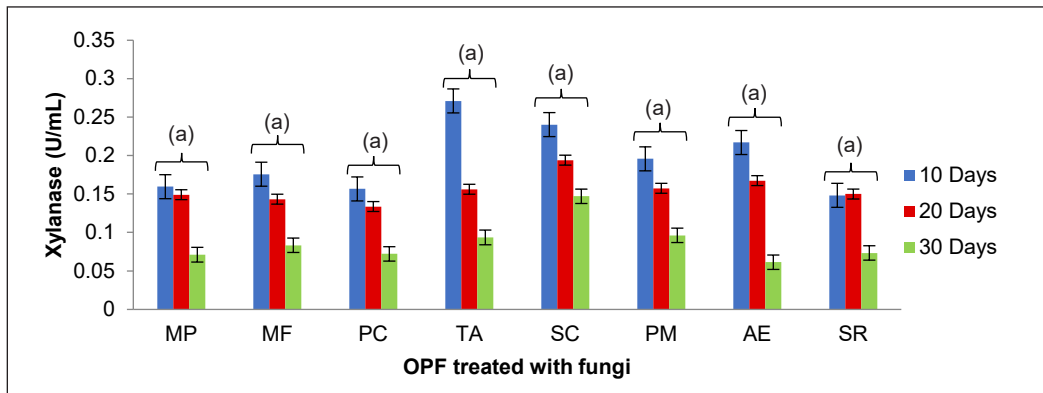

Figure 6. CMCase activity of enzyme extract after OPF pre-treatment with different fungi at 10, 20 and 30 days of incubation (MP = *Marasmius palmivorus;* MF = *Mucor fusiformis*; PC = *Penicillium citrinum*; TA = *Trichoderma asperellum;* SC = *Schizophyllum commune;* PM = *Phanerina mellea;* AE = *Aspergillus ellipticus*; SR = *Syncephalastrum racemosum*)

Figure 7. Avicelase activity of enzyme extract after OPF pre-treatment with different fungi at 10, 20 and 30 days of incubation (MP = *Marasmius palmivorus;* MF = *Mucor fusiformis*; PC = *Penicillium citrinum*; TA = *Trichoderma asperellum;* SC = *Schizophyllum commune;* PM = *Phanerina mellea;* AE = *Aspergillus ellipticus*; SR = *Syncephalastrum racemosum*)

Figure 8. Xylanase activity of enzyme extract after OPF pre-treatment with different fungi at 10, 20 and 30 days of incubation (MP = *Marasmius palmivorus;* MF = *Mucor fusiformis*; PC = *Penicillium citrinum*; TA = *Trichoderma asperellum;* SC = *Schizophyllum commune;* PM = *Phanerina mellea;* AE = *Aspergillus ellipticus*; SR = *Syncephalastrum racemosum*)

Selection of Fungi

The selection of the most favorable fungi for pre-treatment of OPF was based on the average enzyme activity determination results. Figure 9 shows a scatterplot graph of the average ligninolytic enzyme activity against the total cellulolytic + hemicellulolytic enzyme activity. From the graph, *P. mellea* is plotted at the top of the graph (red circle), which shows that the fungi have the highest ligninolytic enzyme activity with low cellulolytic and hemicellulolytic enzyme activity. The ratio between ligninolytic enzyme, which is the desired enzyme, and cellulolytic + hemicellulolytic are best shown by *P. mellea*. It is followed by *S. commune*, located lower than *P. mellea*. *Phanerina mellea* shows the highest average ligninolytic enzyme activity with a value of 0.37 U/mL and an average cellulolytic + hemicellulolytic of 0.18 U/mL. It is followed by *S. commune,* the average ligninolytic
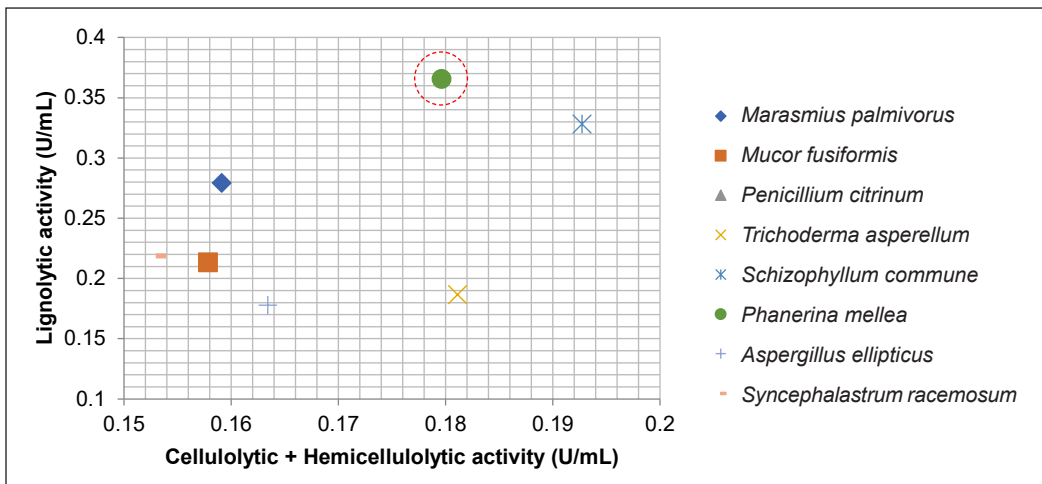
Figure 9. Graph of average ligninolytic enzyme activity against total average cellulolytic and hemicellulolytic enzyme activity of fungi. *Note.* The red circle shows *Phanerina mellea* is plotted at the top of the graph

enzyme activity is 0.33 U/mL, and the average cellulolytic + hemicellulolytic is 0.19 U/mL. In this experiment, *P. mellea* was the most desired fungi for the pre-treatment of OPF.

Selection of the Optimal Ligninolytic Enzyme Activity Production Time

Table 1 shows the average enzyme activity of fungi at different treatment times based on the type of enzyme that was experimented with. The average laccase enzyme activity shows that day 20 has the highest enzyme activity compared to days 10 and 30 of SSF. However, there is no significant difference among days 10, 20, and 30 of SSF ($p>0.05$). For average LiP and MnP enzyme activity, day 10 shows the highest activity, followed by days 20 and 30. However, no significant difference ($p>0.05$) exists between days 10 and 20. It also shows no significant difference between days 20 and 30. However, day 10 is significantly different from day 30 of SSF.

The mean CMCase enzyme activity of day 20 shows the highest activity, followed by days 10 and 30. Days 10, 20, and 30 significantly differ ($p<0.05$) between each treatment time. Like CMCase, average avicelase enzyme activity also shows that day 20 has the highest activity compared to days 10 and 30. There is no significant difference ($p>0.05$) between days 20 and 30 of SSF. However, day 10 significantly differs ($p<0.05$) from days 20 and 30. The mean xylanase enzyme activity of day 10 shows the highest activity, followed by days 20 and 30. The variance analysis shows that day 10 has no significant difference ($p>0.05$) from day 20. However, day 30 significantly differs ($p<0.05$) from days 10 and 20 of SSF.

On average, ligninolytic and hemicellulolytic enzyme activity showed the highest activity on day 10 of SSF, while cellulolytic enzyme activity showed the highest activity

on day 20 of SSF. This study needed ligninolytic enzymes for lignin degradation with minimum cellulolytic and hemicellulolytic enzymes. Therefore, the optimum OPF pre-treatment time is day 10 of SSF.

Table 1
Average enzyme activity of fungi identified on days 10, 20 and 30 of solid-state fermentation

Treatment time (Days)	Average enzyme activity (U/mL)					
	Laccase	LiP	MnP	CMCase	Avicelase	Xylanase
10	0.06[a]	0.52[b]	0.43[b]	0.10[b]	0.24[a]	0.20[b]
20	0.10[a]	0.32[ab]	0.35[ab]	0.19[c]	0.30[b]	0.16[b]
30	0.06[a]	0.15[a]	0.25[a]	0.03[a]	0.20[a]	0.09[a]
SEM	0.01	0.09	0.04	0.04	0.02	0.09
p-Value	0.75	<0.001	0.01	<0.001	<0.001	<0.001

Note: Means that do not share a letter are significantly different, where (P < 0.05) is considered a significant value

DISCUSSION

The different coloration and colony structure indicated the differences between each fungus. Some fungi can easily be noticed based on their morphological structure in nature. For example, the fungi filamentous structure is shown in the cottony fibrous structure of hyphae with cellulose-enriched materials (Mäkelä et al., 2020). The white concentric rings of F14, F39, and F49 are synonymous with WRF (Abdel-Hamid et al., 2013). F03, F32, F77, F65, and F02 are brown or soft rot fungi.

Each species identified in this study has its specialties. Some fungi species are used in commercial industries, and some are still under investigation. For example, *M. palmivorus* pre-treatment on empty fruit bunches (EFB) and palm kernel meal (PKM) did not improve the growth of larvae of the Black Soldier Fly (BSF) (Colombatto et al., 2003). *Mucor fusiformis* or *Zygorhynchus psychrophilus* is a fungus usually used in food manufacturing, such as cheese and tofu. However, it is infectious and dangerous to human health (Walther et al., 2013). *Penicillium citrinum* is used in β-mannanase enzyme production and industrial applications, including animal feed production (Lima et al., 2021). *Schizophyllum commune* is used in rice straw fermentation to produce high levels of xylanase enzyme under the state fermentation method for the pre-bleaching of ethanol-soda pulp (Gautam et al., 2018).

Phanerina mellea is also a WRF commonly called *Ceriporia mellea* (Miettinen et al., 2016). The information on this fungus is limited, and its enzyme activity production and application have never been investigated. *Aspergillus ellipticus* is a well-known wood-decaying fungus, and various studies have used this fungus in cellulose production studies. This fungus is usually used in pharmaceuticals, food ingredients and enzyme production (Gupte & Madamwar, 1997).

Ahmad Fariz Nicholas, Hasliza Abu Hassim, Mohd Huzairi Mohd Zainudin, Zunita Zakaria,
Mohd Termizi Yusof, Mohd Nazri Md Nayan and Amirul Faiz Mohd Azmi

In this enzyme activity determination study, some fungi lacked laccase enzyme activities as some physiological fungi groups were never reported to produce laccase enzyme, such as *zygomycetes,* which is the division of *M. fusiformis* (Mäkelä et al., 2020). Gupte et al. (2007) reported no laccase activity in *P. chrysosporium*. *Fusarium verticillioides* and *Aspergillus niger* secreted no laccase enzyme activity in the study reported by Pant and Adholeya (2007). Enzyme production by fungi can be classified into three categories which are fungi that secret laccase and two peroxidases (MnP, LiP), laccase and one peroxidase, and laccase or peroxidase only (Wang et al., 2019). *Mucor fusiformis* and *A. elepticus* are classified into fungi that secret laccase and one peroxidase.

Lignin peroxidase resulted in the highest enzyme activity in the 0.08 – 0.90 U/mL range, with the highest recorded by *P. mellea* on day 10 of SSF. It is lower compared to LiP enzyme activity produced by *P. chrysosporium* with 14.25 U/mL on day 10 of SSF with wheat straw as the substrate, as reported by Gupte et al. (2007). The difference in LiP enzyme activity production between these two studies could be caused by the different substrates, nutrient supplementation and even the inoculation number used. In this study, three inoculums were used, but they used five inoculums in their SSF.

In general, most of the fungi identified in this study produced higher MnP enzyme activity than laccase and lower than LiP enzyme. The low supplementation of manganese (II) ion, which is highly reactive and was used to avoid MnP, hindered LiP enzyme production (Hofrichter, 2002).

Cellulolytic enzyme activity showed a similar value and trend for all fungi identified with day 20 showed the highest activity compared to days 10 and 30 of SSF. The peak time production of cellulolytic enzyme was delayed compared to ligninolytic enzyme. The physiological structure of the OPF, which is covered with the cell wall structure, induces the production of ligninolytic enzymes first before WRF produces cellulolytic and hemicellulolytic enzymes. The WRF colonized the cell lumina of the OPF before the fungal mycelia propagated the cell wall structure by the Fenton reaction. This event caused the fungi to produce ligninolytic enzyme first before cellulolytic enzyme (Dong et al., 2013; Ji et al., 2014; Rouches et al., 2016). It was also shown by Rahman et al. (2011) that *P. chrysosporium* secretes the ligninolytic enzyme before the cellulolytic enzyme, resulting in lower sugar production compared to *A. terreus*. The activity decreased on day 30 as the cellulolytic enzyme activity was suppressed, and delignification happened, producing water.

In the selection of fungi, filamentous fungi that produced high ligninolytic enzymes with low cellulolytic + hemicellulolytic enzyme activity will be selected for further study. Ligninolytic enzymes are responsible for delignification (Saha et al., 2016). Narayanazwamy et al. (2013) reported that lignin degradation involves extracellular enzymes (LiP, MnP and laccase). The lignin degradation ability of filamentous fungi is

the critical factor in the pre-treatment. However, cellulose recovery to conserve the total availability of glucose used by animals will determine the fungi's actual potential ability (Tian et al., 2012). *Phanerina mellea* showed the highest ligninolytic enzyme activity with low cellulolytic and hemicellulolytic enzyme activity.

The optimal ligninolytic enzyme production time was determined based on the average enzyme activity of fungi identified on days 10, 20 and 30 of SSF. In this study, each fungus showed various laccase enzyme activities. The production of laccase enzyme activity is different for different fungi strains. Isroi et al. (2011) stated that one of the factors that influenced the production of ligninolytic enzyme production was the fungi strain. The study by Gupte et al. (2007) also reported that the production of enzyme activity by *T.versicolor*, *P.crysosporium*, *P.ostreatus,* and *I. lateus* on wheat straw showed the highest on day 10 of SSF. Akpinar and Urek (2012) also reported that the highest laccase enzyme production time by *Pleurotus eryngii* is on day 10 of SSF.

CONCLUSION

WRF has the potential to be used in the biological pre-treatment of lignocellulosic materials. With the SSF technique, the enzyme activity of WRF was successfully detected and analyzed, as well as their ability to degrade lignin in OPF. The average ligninolytic enzyme activity was higher than the average cellulolytic + hemicellulolytic enzyme activity. *P. mellea* best showed the enzyme activity production of the desired enzyme. *P. mellea* showed an average ligninolytic enzyme activity value of 0.37 U/mL; the average cellulolytic + hemicellulolytic is 0.18 U/ml. *P. mellea* can be further used for pre-treatment OPF in animal feed production. The optimal pre-treatment time of OPF was also successfully analyzed. Day 10 of SSF showed the best pre-treatment time for producing high ligninolytic enzyme activity.

ACKNOWLEDGEMENTS

REFERENCES

Abdel-Hamid, A. M., Solbiati, J. O., & Cann, I. K. (2013). Insights into lignin degradation and its potential industrial applications. *Advances in Applied Microbiology*, *82,* 1–28. https://doi.org/10.1016/B978-0-12-407679-2.00001-6

Akpinar, M., & Urek, R. O. (2012). Production of ligninolytic enzymes by solid-state fermentation using *Pleurotus eryngii*. *Preparative Biochemistry and Biotechnology, 42*(6), 582–597. https://doi.org/10.108 0/10826068.2012.673528

Asgher, M., Bhatti, H. N., Ashraf, M., & Legge, R. L. (2008). Recent developments in biodegradation of industrial pollutants by white rot fungi and their enzyme system. *Biodegradation, 19*(6), 771-783. https://doi.org/10.1007/s10532-008-9185-3

Azmi, M. A., Yusof, M. T., Zunita, Z., & Hassim, H. A. (2019). Enhancing the utilization of oil palm fronds as livestock feed using biological pre-treatment method. *IOP Conference Series: Earth and Environmental Science*, *230*(1)*,* Article 12077. https://doi.org/10.1088/1755-1315/230/1/012077

Buayairaksa, M., Kanokmedhakul, S., Kanokmedhakul, K., Moosophon, P., Hahnvajanawong, C., & Soytong, K. (2011). Cytotoxic lasiodiplodin derivatives from the fungus *Syncephalastrum racemosum*. *Archives of Pharmacal Research, 34*(12), 2037–2041. https://doi.org/10.1007/s12272-011-1205-x

Chanjula, P., Petcharat, V., & Cherdthong, A. (2017). Effects of fungal (Lentinussajor-caju) treated oil palm frond on performance and carcass characteristics in finishing goats. *Asian-Australasian Journal of Animal Sciences, 30*(6), Article 811. https://doi.org/10.5713/ajas.16.0704

Chandran, B., & Nigam, P. (2001). Studies on the production of enzymes by white-rot fungi for the decolourisation of textile dyes. *Enzyme and Microbial Technology, 29*(8-9), 575–579. https://doi.org/10.1016/S0141-0229(01)00430-6

Colombatto, D., Morgavi, D. P., Furtado, A. F., & Beauchemin, K. A. (2003). Screening of exogenous enzymes for ruminant diets: Relationship between biochemical characteristics and in vitro ruminal degradation. *Journal of Animal Science, 81*(10), 2628–2638. https://doi.org/10.2527/2003.81102628x

Dinis, M. J., Bezerra, R. M. F., Nunes, F., Dias, A. A., Guedes, C. V, Ferreira, L. M. M., Cone, J. W., Marques, G. S. M., Barros, A. R. N., & Rodrigues, M. A. M. (2009). Bioresource Technology Modification of wheat straw lignin by solid state fermentation with white-rot fungi. *Bioresource Technology*, *100*(20), 4829–4835. https://doi.org/10.1016/j.biortech.2009.04.036

Dong, X. Q., Yang, J. S., Zhu, N., Wang, E. T., & Yuan, H. L. (2013). Sugarcane bagasse degradation and characterization of three white-rot fungi. *Bioresource Technology, 131,* 443–451. https://doi.org/10.1016/j.biortech.2012.12.182

Falade, A. O., Nwodo, U. U., Iweriebor, B. C., Green, E., Mabinya, L. V., & Okoh, A. I. (2017). Lignin peroxidase functionalities and prospective applications. *MicrobiologyOpen, 6*(1), Article e00394. https://doi.org/10.1002/mbo3.394

Galal, F. H., AbuElnasr, A., Abdallah, I., Zaki, O., & Seufi, A. M. (2017). Culex (Culex) pipiens mosquitoes carry and harbor pathogenic fungi during their developmental stages. *Journal of Clinical Practice and Research, 39*(1), 1-6. https://doi.org/10.5152/etd.2017.16067

Gautam, A., Kumar, A., Bharti, A. K., & Dutt, D. (2018). Rice straw fermentation by *Schizophyllum commune* ARC-11 to produce high level of xylanase for its application in pre-bleaching. *Journal of Genetic Engineering and Biotechnology, 16*(2)*,* 693–701. https://doi.org/10.1016/j.jgeb.2018.02.006

Ghani, A. A. A., Rusli, N. D., Shahudin, M. S., Goh, Y. M., Zamri-Saad, M., Hafandi, A., & Hassim, H. A. (2017). Utilisation of oil palm fronds as ruminant feed and its effect on fatty acid metabolism. *Pertanika Journal of Tropical Agricultural Science, 40*(2), 215-224.

Gupte, A., & Madamwar, D. (1997). Production of cellulolytic enzymes by coculturing of *Aspergillus* ellipticus and *Aspergillus* fumigatus grown on bagasse under solid state fermentation. *Applied Biochemistry and Biotechnology, 62,* 267–274. https://doi.org/10.1007/BF02788002

Gupte, A., Gupte, S., & Patel, H. (2007). Ligninolytic enzyme production under solid-state fermentation by white rot fungi. *Journal of Scientific and Industrial Research 66*(08), 611–14.

Hofrichter, M. (2002). Lignin conversion by manganese peroxidase (MnP). *Enzyme and Microbial Technology, 30*(4), 454–466. https://doi.org/10.1016/S0141-0229(01)00528-2

Hu, H. L., Brink, J. Van Den, Gruben, B. S., Wösten, H. A. B., Gu, J., & Vries, R. P. De. (2011). International biodeterioration & biodegradation improved enzyme production by co-cultivation of *Aspergillus niger* and *Aspergillus oryzae* and with other fungi. *International Biodeterioration & Biodegradation, 65*(1), 248–252. https://doi.org/10.1016/j.ibiod.2010.11.008

Islam, M., Dahlan, I., Rajion, M. A., & Jelan, Z. A. (2000). Productivity and nutritive values of different fractions of oil palm (Elaeis guineensis) frond. *Asian-Australasian Journal of Animal Sciences, 13*(8), 1113–1120. https://doi.org/10.5713/ajas.2000.1113

Isroi, I., Millati, R., Niklasson, C., Cayanto, C., Taherzadeh, M. J., & Lundquist, K. (2011). Biological treatment of lignocelluloses with white-rot fungi and its applications. *BioResources, 6*(4), 5224–5259.

Ji, L., Yang, J., Fan, H., Yang, Y., Li, B., Yu, X., Zhu, N., & Yuan, H. (2014). Synergy of crude enzyme cocktail from cold-adapted Cladosporium cladosporioides Ch2-2 with commercial xylanase achieving high sugars yield at low cost. *Biotechnology for Biofuels, 7*(1), Article 130. https://doi.org/10.1186/s13068-014-0130-x

Khan, S. A., Hamayun, M., Yoon, H., Kim, H. Y., Suh, S. J., Hwang, S. K., Kim, J. M., Lee, I. J., Choo, Y. S., Yoon, U. H., Kong, W. S., Lee, B. M., & Kong, W. S. (2008). Plant growth promotion and *Penicillium citrinum*. *BMC Microbiology, 8*(1), Article 231. https://doi.org/10.1186/1471-2180-8-231

Kumar, A., & Arora, P. K. (2022). Biotechnological applications of manganese peroxidases for sustainable management. *Frontiers in Environmental Science, 10,* Article 875157. https://doi.org/10.3389/fenvs.2022.875157

Lima, A. C., Silva, D., Silva, V., Godoy, M., Cammarota, M., & Gutarra, M. (2021). β-Mannanase production by *Penicillium citrinum* through solid-state fermentation using açaí residual biomass (Euterpe oleracea). *Journal of Chemical Technology & Biotechnology, 96*(10), 2744–2754. https://doi.org/10.1002/jctb.6818

Madhavi, V., & Lele, S. S. (2009). Laccase: Properties and applications. *BioResources, 4*(4), 1-24.

Mäkelä, M. R., Hildén, K. S., & Kuuskeri, J. (2020). Fungal lignin-modifying peroxidases and H2O2-producing enzymes. In O. Zaragoza & A. Casdevall (Eds.) *Encyclopedia of Mycology* (pp. 247-259). Elsevier.

Manavalan, T., Manavalan, A., & Heese, K. (2015). Characterization of lignocellulolytic enzymes from white-rot fungi. *Current Microbiology, 70*(4), 485–498. https://doi.org/10.1007/s00284-014-0743-0

Mahmood, Z. A., & Azhar, I. (2017). Detection of aflatoxins and use of scanning electron microscope for the identification of fungal species in some commonly used spices. *Asian Journal of Plant Science and Research, 7*(5), 64–73.Miettinen, O., Spirin, V., Vlasák, J., Rivoire, B., Stenroos, S., & Hibbett, D. (2016).
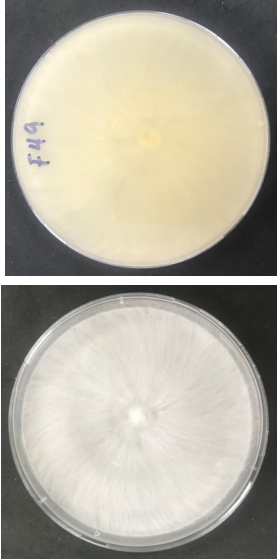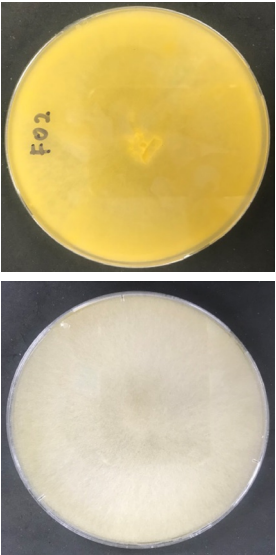
Polypores and genus concepts in Phanerochaetaceae (Polyporales, Basidiomycota). *MycoKeys, 17,* 1-46. https://doi.org/10.3897/mycokeys.17.10153

Pant, D., & Adholeya, A. (2017). Enhanced production of ligninolytic enzymes and decolorization of molasses distillery wastewater by fungi under solid-state fermentation. *Biodegradation, 18*, 647–659. https://doi.org/10.1007/s10532-006-9097-z

Ohm, R. A., Jong, J. F. De, Lugones, L. G., Aerts, A., Kothe, E., Stajich, J. E., de Vries, R. P., Record, E., Levasseur, A., Baker, S. E., Bartholomew, K. A., Coutinho, P. M., Erdmann, S., Fowler, T. J., Gathman, A. C., Lombard, V., Henrissat, B., Knabe, N., Kües, U., … & Wösten, H. A. B. (2010). Genome sequence of the model mushroom *Schizophyllum commune*. *Nature Biotechnology, 28*(9), 957-963. https://doi.org/10.1038/nbt.1643

Parveez, G. K. A., Kamil, N. N., Zawawi, N. Z., Ong-Abdullah, M., Rasuddin, R., Loh, S. H., Selvadaray, K. R., Hoong, S. S., & Idris, Z. (2022). Oil palm economic performance in Malaysia and R&D progress in 2021. *Journal of Oil Palm Research, 34*(2), 185–218. https://doi.org/10.21894/jopr.2022.0036

Pham, M. T., Huang, C. M., & Kirschner, R. (2019). First report of the oil palm disease fungus *Marasmius palmivorus* from Taiwan causing stem rot disease on native Formosa palm *Arenga engleri* as new host. *Letters in Applied Microbiology, 70*(3), 143-150. https://doi.org/10.1111/lam.13257

Podder, D., & Ghosh, S. K. (2019). A new application of *Trichoderma asperellum* as an *Anopheline larvicide* for eco friendly management in medical science. *Scientific Reports, 9*(1), Article 1108. https://doi.org/10.1038/s41598-018-37108-2

Rahman, M. M., Lourenço, M., Hassim, H. A., Baars, J. J., Sonnenberg, A. S., Cone, J. W., Boever, J. D., & Fievez, V. (2011). Improving ruminal degradability of oil palm fronds using white rot fungi. *Animal Feed Science and Technology, 169*(3-4), 157–166. https://doi.org/10.1016/j.anifeedsci.2011.06.014

Raju, B., Santhanakumar, K. S., & Kesavachandran, U. (2020). Gastrointestinal involvement of unusual *Mucormycete*, *Syncephalastrum racemosum* in a diabetic patient with adenocarcinoma: Rare case presentation with review of literature. *Infection, 48*, 791–797. https://doi.org/10.1007/s15010-020-01455-y

Rouches, E., Herpoël-Gimbert, I., Steyer, J. P., & Carrere, H. (2016). Improvement of anaerobic degradation by white-rot fungi pretreatment of lignocellulosic biomass: A review. *Renewable and Sustainable Energy Reviews, 59,* 179–198. https://doi.org/10.1016/j.rser.2015.12.317

Rusli, N. D., Azmi, M. A., Mat, K., Hasnita, C. H., Wan-Zahari, M., Azhar, K., Zamri-Saad, M., & Hassim, H. A. (2019). The effect of physical and biological pre-treatments of oil palm fronds on in vitro ruminal degradability. *Pertanika Journal of Tropical Agricultural Science, 42*(2), 791-805.

Rusli, N. D., Ghani, A. A. A., Mat, K., Yusof, M. T., Zamri-Saad, M., & Hassim, H. A. (2021). The potential of pretreated oil palm frond in enhancing rumen degradability and growth performance: A review. *Advances in Animal and Veterinary Sciences, 9*(6), 811–822. http://dx.doi.org/10.17582/journal.aavs/2021/9.6.811.822

Saha, B. C., Qureshi, N., Kennedy, G. J., & Cotta, M. A. (2016). Biological pretreatment of corn stover with white-rot fungus for improved enzymatic hydrolysis. *International Biodeterioration & Biodegradation, 109,* 29–35. https://doi.org/10.1016/j.ibiod.2015.12.020

Saif, F. A., Yaseen, S. A., Alameen, A. S., Mane, S. B., & Undre, P. B. (2020). Identification of *Penicillium* species of fruits using morphology and spectroscopic methods. *In Journal of Physics: Conference Series*, *1644*, Article 12019. https://doi.org/10.1088/1742-6596/1644/1/012019

Saminathan, M., Mohamed, W. N. W., Noh, A. M., Ibrahim, N. A., Fuat, M. A., Ramiah, S. K., Chung, E. L. T., & Dian, N. L. H. M. (2012). Treated oil palm frond and its utilisation as an improved feedstuff for ruminants-An overview. *Journal of Oil Palm Research, 34*(4)*,* 591–607. https://doi.org/10.21894/jopr.2021.0041

Sigler, L., Bartley, J. R., Parr, D. H., & Morris, A. J. (1999). Maxillary Sinusitis Caused by Medusoid Form ofSchizophyllum commune. *Journal of Clinical Microbiology, 37*(10), 3395–3398.

Sukri, S. M., Rahman, R. A., Illias, R. M., & Yaakob, H. (2014). Optimization of alkaline pretreatment conditions of oil palm fronds in improving the lignocelluloses contents for reducing sugar production. *Biotechnology Letter, 19*(1), 9006–9018.

Tamur, H. A., Al-Janabi, H. J., Al-Janabi, J. K. A., Mohsin, L. Y., & Al-Yassiry, Z. A. N. (2019). Characterization and antagonistic activity of new causal agent of wilt disease in *Imperata cylindrica* (*Marasmius palmivorus*). *Journal of Pure and Applied Microbiology, 13*(3), 1525–1536. https://doi.org/10.22207/JPAM.13.3.24

Tian, X. F., Fang, Z., & Guo, F. (2012). Impact and prospective of fungal pre-treatment of lignocellulosic biomass for enzymatic hydrolysis. *Biofuels, Bioproducts and Biorefining, 6*(3)*,* 335–350. https://doi.org/10.1002/bbb.346

Toth, G. B., & Pavia, H. (2000). Removal of dissolved brown algal phlorotannins using insoluble polyvinylpolypyrrolidone (PVPP). *Journal of Chemical Ecology, 27,* 1899–1910. https://doi.org/10.1023/A:1010421128190

Tuyen, D. V., Phuong, H. N., Cone, J. W., Baars, J. J. P., Sonnenberg, A. S. M., & Hendriks, W. H. (2013). Effect of fungal treatments of fibrous agricultural by-products on chemical composition and in vitro rumen fermentation and methane production. *Bioresource Technology, 129,* 256–263. https://doi.org/10.1016/j.biortech.2012.10.128

Verma, M., Brar, S. K., Tyagi, R. D., Surampalli, R. Y., & Val, J. R. (2007). Antagonistic fungi, *Trichoderma spp*. Panoply of Biological Control, 37*, 1–20. https://doi.org/10.1016/j.bej.2007.05.012

Walther, G., Pawłowska, J., Alastruey-Izquierdo, A., Wrzosek, M., Rodriguez-Tudela, J. L., Dolatabadi, S., Chakrabarti, A., & Hoog, G. S. D. (2013). DNA barcoding in Mucorales: An inventory of biodiversity. *Persoonia: Molecular Phylogeny and Evolution of Fungi, 30*(1), 11-47. https://doi.org/10.3767/003158513X665070

Wang, F., Xu, L., Zhao, L., Ding, Z., Ma, H., & Terry, N. (2019). Fungal laccase production from lignocellulosic agricultural wastes by solid-state fermentation: A review. *Microorganisms, 7*(12)*,* Article 665. https://doi.org/10.3390/microorganisms7120665

Zafar, A. M., Najma, S., Farhana, T., Shahlla, I., Safia, A., Iqbal, A. (2017). Detection of aflatoxins and use of scanning electron microscope for the identification of fungal species in some commonly used spices. *Asian Journal of Plant Science and Research, 7*(5), 64–73.

APPENDICES

Supplementary Tables

Table S1
Fungi identified species with the characteristics

No	Sample Name	Scientific Name	Front	Back	Characteristics
1	F49	*Marasmius palmivorus*			• Mushroom-forming fungi • Division: *Basidiomycota* • Causing white rot • Mainly in monocots and particularly oil and coconut palms • Produced disease symptoms and death of non-wounded Formosa palm tree (Pham et al., 2019)
2	F02	*Mucor fusiformis*			• Epithet: Fusiformis • Other name: *Zygorhynchus psychrophilus*. • Division: *Zygomycota*. • Filamentous fungi. • Saprotroph organisms inhabiting dead plant material, soil and dung. • Used in the fermentation of tempeh or tofu. • Used in the production of several cheeses. • Responsible for spoiling fresh and manufactured food. • Involved in human infection (Walther et al., 2013)
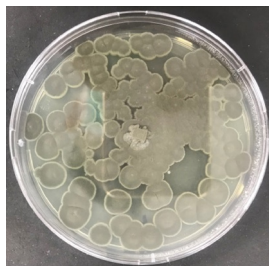
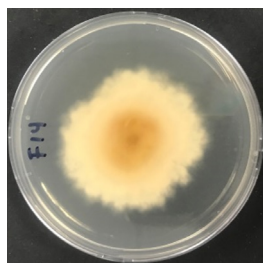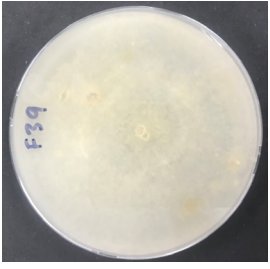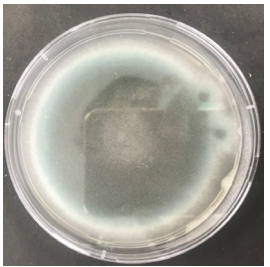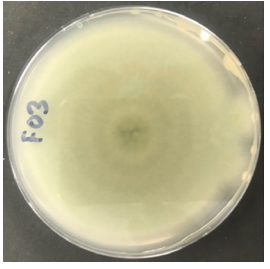| No.	Code	Images	Description
3	F77	*Penicillium citrinum* — Back / Front	• Division: *Ascomycota* • Common Endophytic fungus of cereal plants. • Benefits to the host plant include increased tolerance to herbivory, disease, heat, salt, and drought, as well as increased below and above-ground biomass (Khan et al., 2008)
4	F32	*Trichoderma asperellum* — Back / Front	• Division: *Ascomycota*. • Causing soft-rot. • Used commercially and experimentally as a biopesticide and biocontrol agent. • Well known as rivalry for several soil phytopathogens, including other fungi, bacteria and invertebrates. • Help with other plant growth (domestic and greenhouse plants and crops) (Verma et al., 2007)
5	F14	*Schizophyllum commune* — Back / Front	• Other Name: Split gill Fungus • Division: *Basidiomycota*. • Causing white rot. • Found on every continent except Antarctica. • The gills function to produce basidiospores. • Can be found on fallen branches and timber of deciduous trees.(Ohm et al., 2010)
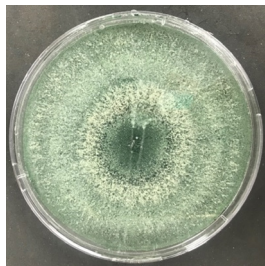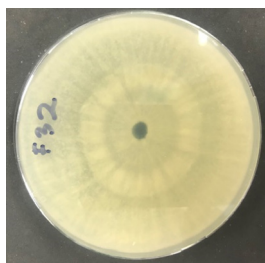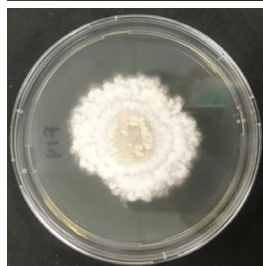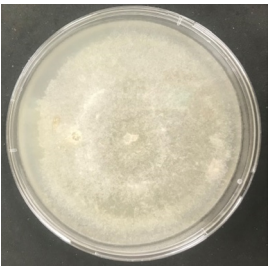
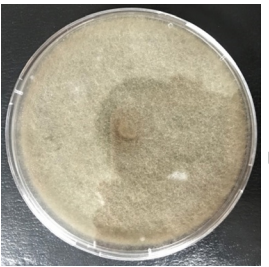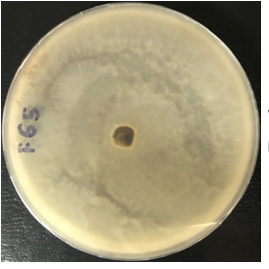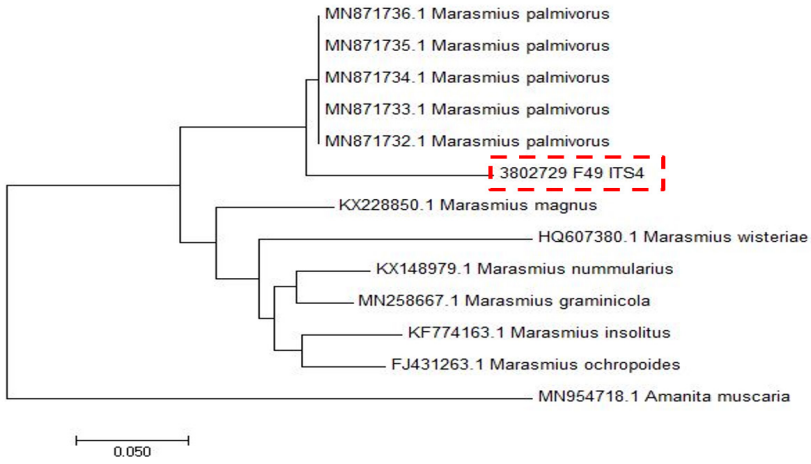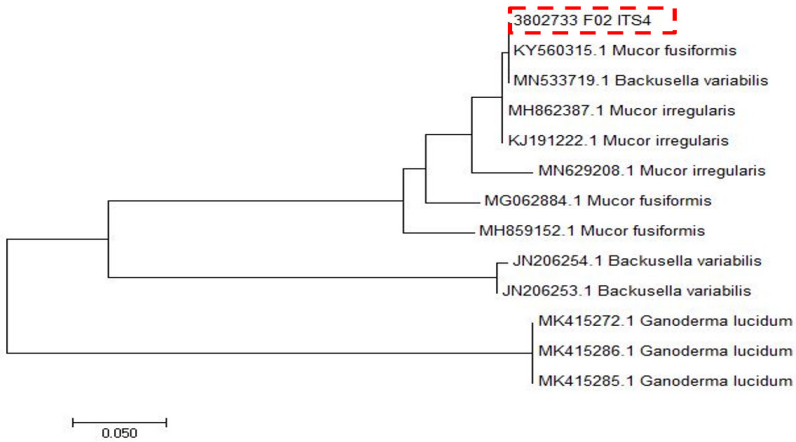| No.	Code	Images	Description
6	F39	*Phanerina mellea* — Front / Back	• Other Name: *Polyporus melleus, Poria mellea, Ceriporia mellea, Gloeoporus melleus.* • Division: *Basidiomycota* • Causing white rot • Genus: *Phanerochaete* • Miettinen et al., 2016
7	F03	*Aspergillus ellipticus* — Front / Back	• Divisions: *Ascomycota* • Other name: *Aspergillus helicothrix.* • Used for pharmaceuticals, food ingredients and enzymes (Hu et al., 2011) • Show a high degree of β-glycosidase activity. • Wood decaying fungi • Synergism between *Aspergillus ellipticus* and *Aspergillus fumigatus* improves hydrolytic and β-glycosidase activity (Gupte & Madamwar, 1997)
8	F65	*Syncephalastrum racemosum* — Front / Back	• Other name: *Syncephalastraceae* • Filamentous fungi • Can cause nail disease • Isolated fungal species of soil in tropical and subtropical regions. • Produce the highest DNase activity. • Used in microbial transformation for hydroxylation of steroids, olivetol, milbemycins, and cinobufagin (Buayairaksa et al., 2011)

Table S2

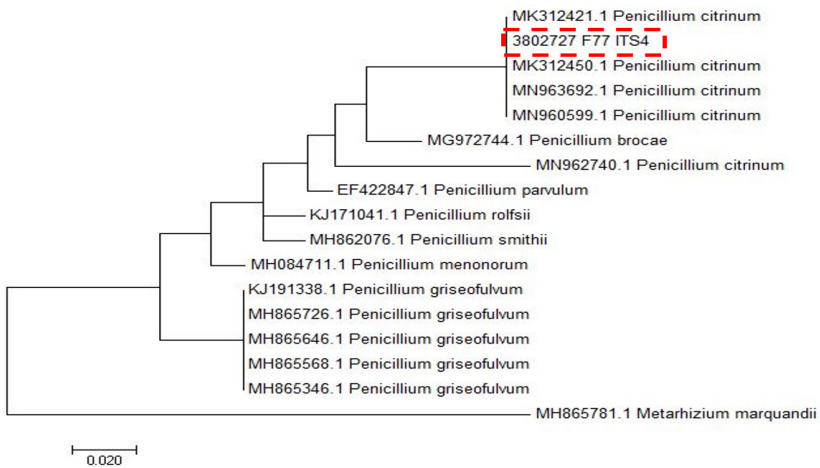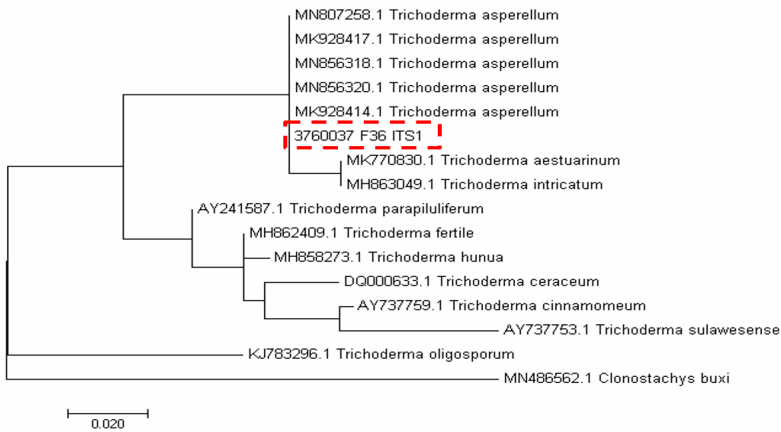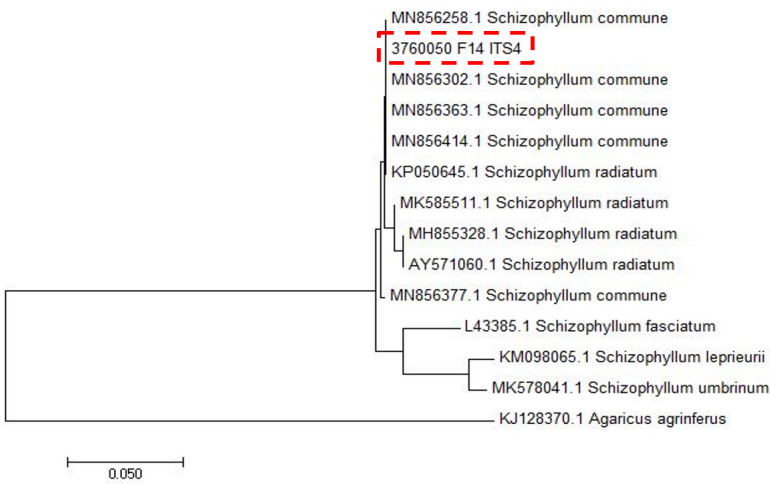*Phylogenetic tree of isolated fungi from OPF sample*

F49

	MN871736.1 Marasmius palmivorus
	MN871735.1 Marasmius palmivorus
	MN871734.1 Marasmius palmivorus
	MN871733.1 Marasmius palmivorus
	MN871732.1 Marasmius palmivorus
	3802729 F49 ITS4
	KX228850.1 Marasmius magnus
	HQ607380.1 Marasmius wisteriae
	KX148979.1 Marasmius nummularius
	MN258667.1 Marasmius graminicola
	KF774163.1 Marasmius insolitus
	FJ431263.1 Marasmius ochropoides
	MN954718.1 Amanita muscaria

0.050

F02

	3802733 F02 ITS4
	KY560315.1 Mucor fusiformis
	MN533719.1 Backusella variabilis
	MH862387.1 Mucor irregularis
	KJ191222.1 Mucor irregularis
	MN629208.1 Mucor irregularis
	MG062884.1 Mucor fusiformis
	MH859152.1 Mucor fusiformis
	JN206254.1 Backusella variabilis
	JN206253.1 Backusella variabilis
	MK415272.1 Ganoderma lucidum
	MK415286.1 Ganoderma lucidum
	MK415285.1 Ganoderma lucidum

0.050

F77

	MK312421.1 Penicillium citrinum
	3802727 F77 ITS4
	MK312450.1 Penicillium citrinum
	MN963692.1 Penicillium citrinum
	MN960599.1 Penicillium citrinum
	MG972744.1 Penicillium brocae
	MN962740.1 Penicillium citrinum
	EF422847.1 Penicillium parvulum
	KJ171041.1 Penicillium rolfsii
	MH862076.1 Penicillium smithii
	MH084711.1 Penicillium menonorum
	KJ191338.1 Penicillium griseofulvum
	MH865726.1 Penicillium griseofulvum
	MH865646.1 Penicillium griseofulvum
	MH865568.1 Penicillium griseofulvum
	MH865346.1 Penicillium griseofulvum
	MH865781.1 Metarhizium marquandii

0.020

Ahmad Fariz Nicholas, Hasliza Abu Hassim, Mohd Huzairi Mohd Zainudin, Zunita Zakaria,
Mohd Termizi Yusof, Mohd Nazri Md Nayan and Amirul Faiz Mohd Azmi
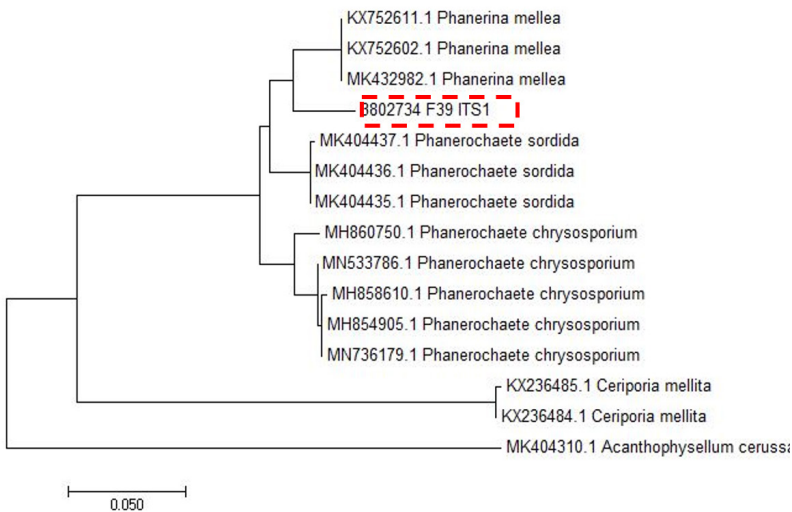
F32

F14

F39

F03

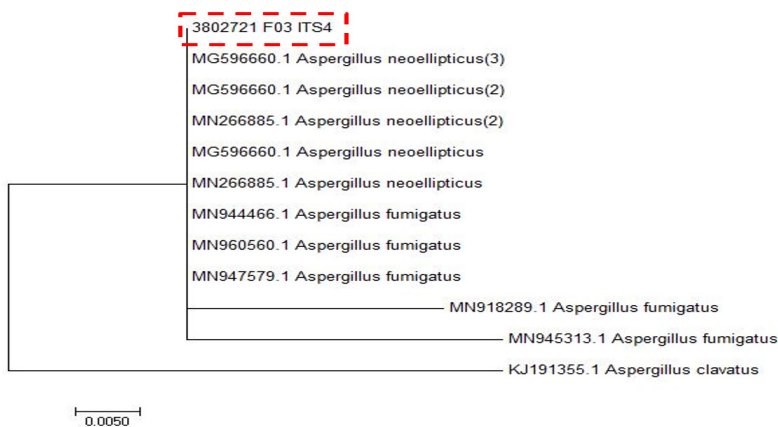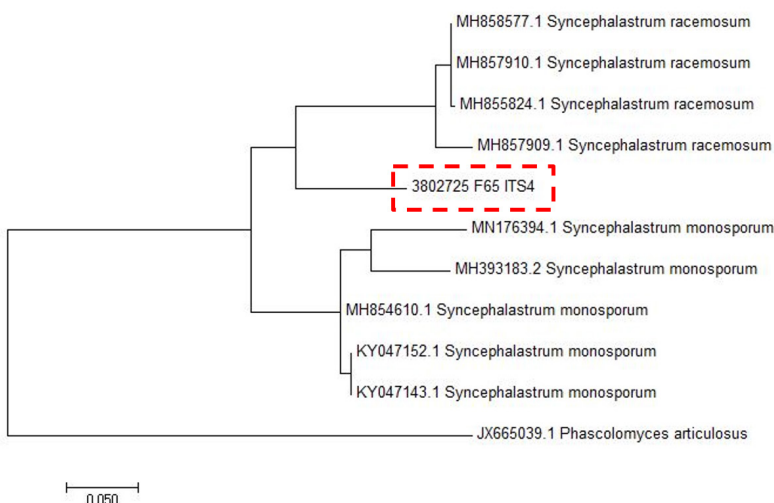**F65**

Table S3
The microscopic structure of S. commune *(a) morphology on PDA agar media, (b) The microscopic structure of* S. commune*, (c) The morphology reference of* S. commune *(Sigler et al., 1999)*
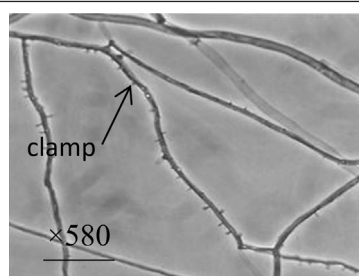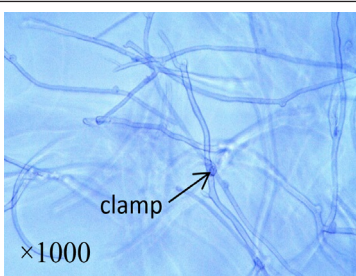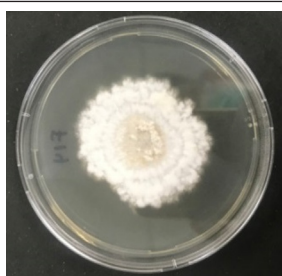
Table S4

The microscopic structure of A. ellipticus *(a) morphology on PDA agar media, (b) The microscopic structure of* A. ellipticus*, (c) SEM image of* A. ellipticus *(Zafar et al., 2017)*
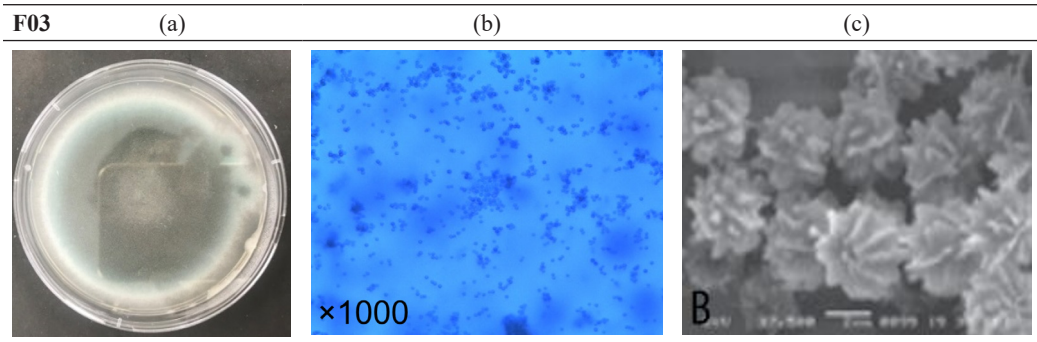
F03	(a)	(b)	(c)

Table S5

The microscopic structure of T. asperellum *(a) morphology on PDA agar media, (b) The microscopic structure of* T. asperellum*, (c) The morphology reference of* T. asperellum *(Podder & Ghosh, 2019)*
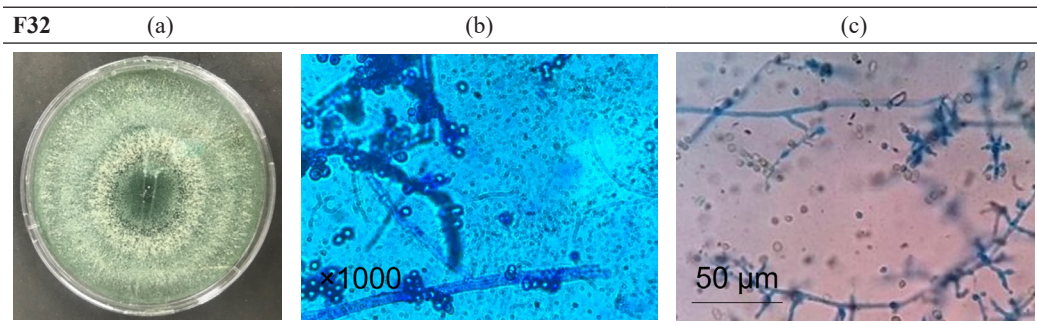
F32	(a)	(b)	(c)

Table S6

The microscopic structure of P. mellea *(a) morphology on PDA agar media, (b) The microscopic structure of* P. mellea *(c) The morphology reference of* P. mellea *(Miettinen et al., 2016)*

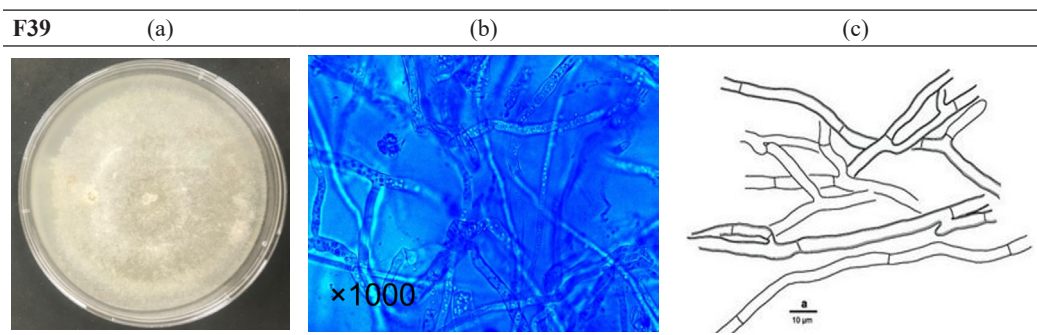| F39	(a)	(b)	(c)

Table S7

The microscopic structure of M. palmivorus *(a) morphology on PDA agar media, (b) The microscopic structure of* M. palmivorus*, (c) The morphology reference of* M. palmivorus *(Tamur et al., 2019)*
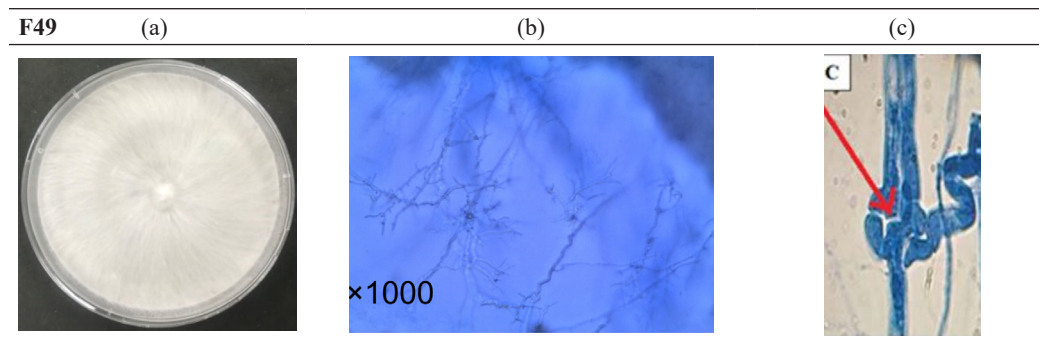
F49	(a)	(b)	(c)

Table S8

The microscopic structure of S. racemosum *(a) morphology on PDA agar media, (b) The microscopic structure of* S. racemosum*, (c) The morphology reference of* S. racemosum *(Raju et al., 2020)*
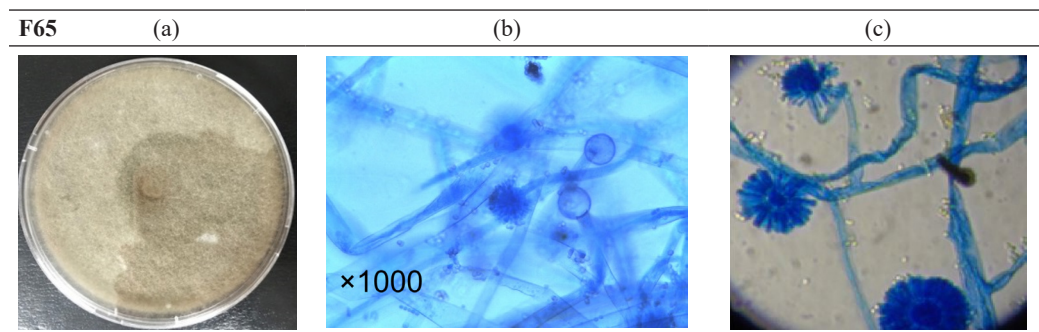
F65	(a)	(b)	(c)

Table S9

The microscopic structure of P. citrinum *(a) morphology on PDA agar media, (b) The microscopic structure of* P. citrinum*, (c) The morphology reference of* P. citrinum *(Saif et al., 2020)*
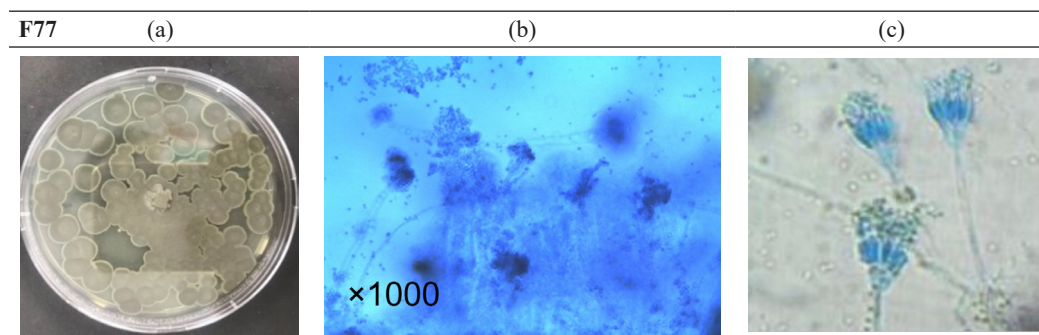
F77	(a)	(b)	(c)

Ahmad Fariz Nicholas, Hasliza Abu Hassim, Mohd Huzairi Mohd Zainudin, Zunita Zakaria,
Mohd Termizi Yusof, Mohd Nazri Md Nayan and Amirul Faiz Mohd Azmi

Table S10

The microscopic structure of M. fusiformis *(a) morphology on PDA agar media, (b) The microscopic structure of* M. Fusiformis*, (c) The morphology reference of* M. fusiformis *(Walther et al., 2013)*

F02	(a)	(b)	(c)